

1

2 Article

3

C₆₀ Bioconjugation with Proteins: Towards a Palette 4 of Carriers for All pH Ranges

5 **Matteo Di Giosia*¹, Francesco Valle², Andrea Cantelli¹, Andrea Bottini¹, Francesco Zerbetto¹
6 and Matteo Calvaresi^{1,*}**7 ¹ Dipartimento di Chimica "G. Ciamician", Università di Bologna, V. F. Selmi 2, 40126 Bologna, Italy;
89 ² Istituto per lo Studio dei Materiali Nanostrutturati (CNR-ISMN), Consiglio Nazionale delle Ricerche, via P.
10 Gobetti 101, 40129 Bologna, Italy; f.valle@ismn.cnr.bo.it
1112 * Correspondence: matteo.digiosia2@unibo.it; matteo.calvaresi3@unibo.it
13

14

15 **Abstract:** The high hydrophobicity of fullerenes and the resulting formation of aggregates in
16 aqueous solutions hamper the possibility of their exploitation in many technological applications.
17 Noncovalent bioconjugation of fullerenes with proteins is an emerging approach for their dispersion
18 in aqueous media. Contrary to covalent functionalization, bioconjugation preserves the
19 physicochemical properties of the carbon nanostructure. The unique photophysical and
20 photochemical properties of fullerenes are then fully accessible for applications in nanomedicine,
21 sensoristic, biocatalysis and materials science fields. And yet, proteins are not universal carriers.
22 Their stability depends on the biological conditions for which they have evolved.23 Here we present two model systems based on pepsin and trypsin. These proteins have opposite net
24 charge at physiological pH. They recognize and disperse C₆₀ in water. UV-Vis spectroscopy, zeta-
25 potential and atomic force microscopy analysis demonstrates that the hybrids are well dispersed
26 and stable in a wide range of pH's and ionic strengths. A previously validated modelling approach
27 identifies the protein binding pocket involved in the interaction with C₆₀. Computational
28 predictions, combined with experimental investigations, provide powerful tools to design tailor-
29 made C₆₀@proteins bioconjugates for specific applications.30 **Keywords:** fullerenes; nanohybrids; nanobiotechnology; bioconjugation; chemical stability
3132

1. Introduction

33 C₆₀, the most representative member of the fullerenes family, has steadily attracted interest for
34 its possible use in various fields, including nanomedicine [1–7]. A plethora of fullerene-based
35 compounds have been synthesized with different targets. They display a range of biological activities
36 that are potentially useful in anticancer therapy, antimicrobial therapy, enzyme inhibition, controlled
37 drug delivery, and contrast or radioactivity-based diagnostic imaging [8–13,7]. Noteworthy is the
38 possibility of their use in photodynamic and photothermal therapies [8,14,15]. The photophysical and
39 electrochemical properties of C₆₀ depend on their dispersion and a strict control of their
40 disaggregation is truly necessary for nanotechnological applications [16,17]. To date two main
41 approaches have been followed to tackle fullerene insolubility in water:

42 i) the covalent approach is the more used method to prevent fullerene aggregation. The benefits
43 obtained by functionalization are often offset by reduced photophysical performances [18];
44 ii) the noncovalent approach requires the use of supramolecular hosts that are amphiphilic molecules
45 able to interact with a single fullerene and to screen it from the aqueous environment. A variety of
46 hosts is capable of interacting with fullerenes. They include surfactants, synthetic polymers,
47 biopolymers, cyclodextrin [19], to name a few. In all cases, they stabilize small clusters of fullerenes
48 [20]. In recent years, also proteins have become used as dispersing agents of fullerenes[21–24], CNTs
49 [25–29] and graphene [30]. Proteins are naturally amphiphilic. This feature may avoid complicated
50 synthetic procedures or the use of organic solvents. Most proteins are also pH responsive, which is
51 an advantage for some manipulations [26]. Steric hindrance and electrostatic repulsion are the key
52 factors determining the stability of the dispersion of carbon nanomaterials-protein complexes in
53 aqueous solutions [31].

54 From the biological point of view, encapsulation of fullerenes by proteins may control and possibly
55 decrease the cytotoxicity. Well-dispersed CNTs are less toxic than their agglomerates [32]. Protein
56 binding can also alter the cellular pathways of interaction with carbon nanomaterials. Ultimately,
57 coating of carbon nanomaterials with proteins can confer them a new biological identity [33].

58 We recently proposed the use of lysozyme to disperse with a 1:1 stoichiometry C₆₀ in water [22]. The
59 hybrid is well-defined and the fullerene binds selectively in the protein-substrate binding pocket. The
60 protein-based supramolecular adduct preserves the photophysical properties of C₆₀ and allows the
61 exploitation of C₆₀ as a photosensitizer for photodynamic treatments [34].

62
63 In this work, we evaluate the stability of C₆₀@protein complexes in biologically relevant conditions.
64 Two proteins characterized by opposite net charges in physiological conditions were used as model
65 systems and the role of the electrostatic contribution to the stability of their adducts with C₆₀ is
66 identified. Applications of docking protocols and MMPBSA calculations [35,36] further provide
67 accurate description of the C₆₀ binding pocket involved in the interaction between protein and C₆₀.
68

69 **2. Materials and Methods**

70 Trypsin from porcine pancreas (Cat. no. T0303), pepsin from porcine gastric mucosa (Cat. no.
71 P7012), fullerene C₆₀ (Cat. no. 483036) were purchased from Sigma Aldrich. They were used without
72 further purifications. Phosphate buffered saline solutions were prepared dissolving the tablets
73 purchased from Sigma Aldrich (Cat. no. P4417) in milliQ water.

74
75 *2.1 C₆₀@Protein Synthesis*

76 The C₆₀@protein hybrids were prepared mixing an excess of fullerene powder with a 0.3 mM
77 solution of each protein (5 mL), with a 2:1 stoichiometry. NaOH and HCl 1M were used to adjust pH
78 of the protein solutions. The heterogeneous mixtures were then sonicated in a vial for 120 minutes
79 using a probe tip ultrasonicator (Hielscher Ultrasonic Processor UP200St, equipped with a sonotrode
80 S26d7, used at 40% of the maximum amplitude). During the process, the sample was refrigerated
81 with an ice bath. The dark brown turbid mixture obtained after the sonication was centrifuged at 10
82 kRCF. The resulting supernatant was then collected and characterized.

83
84 *2.2 C₆₀@Protein Characterization*

85 UV-Vis absorption spectra were recorded at 25 °C by means of Agilent Cary 60 UV-Vis
86 Spectrophotometer. Surface charge analysis of the hybrids were estimated measuring the zeta-
87 potential at 25 °C by means of Malvern Nano ZS.

88 AFM experiments were performed at the SPM@ISMN microscopy facility in Bologna. AFM
89 analysis (Digital Instruments, Multimode VIII equipped with a Nanoscope V) operated in ScanAsyst
90 mode were performed to evaluate the quality of the monodispersion of the bioconjugates. The

91 samples were prepared by drop casting 10 μ L of C_{60} @protein solution onto a freshly cleaved mica
92 substrate for 10 minutes then rinsed with milliQ water and dried under nitrogen flux/stream.

93 *2.3 Computational protocol*

94 **Generation of the poses.** Docking models were obtained using the PatchDock algorithm [37].
95 PatchDock takes as input two molecules and computes three-dimensional transformations of one of
96 the molecules with respect to the other with the aim of maximizing surface shape complementarity,
97 while minimizing the number of steric clashes.

98 **Scoring of the poses.** Accurate rescoring of the complexes is then carried out using FireDock
99 program [38]. This method simultaneously targets the problem of flexibility and scoring of solutions
100 produced by fast rigid-body docking algorithms. Sidechain flexibility is modeled by rotamers and
101 Monte Carlo minimization [39]. Following the rearrangement of the side-chains, the relative position
102 of the docking partners is refined by Monte Carlo minimization of the binding score function. Free
103 energy of solvation/desolvation in the binding process is taken into account by a solvation model that
104 uses estimated effective atomic contact energies (ACE) [40]. All the candidates are ranked by a
105 binding score [40]. This score includes, in addition to atomic contact energy used to estimate the
106 desolvation energies [40], van der Waals interactions, partial electrostatics, explicit hydrogen and
107 disulfide bonds contribution. In addition, three components to the total binding score are added: $E_{\pi-\pi}$
108 for the calculation of the $\pi-\pi$ interactions, $E_{\text{cation}-\pi}$ for the calculation of the cation- π interactions and
109 E_{aliph} for the calculation of hydrophobic interactions.

110 **Minimizing the pose.** The best poses for every selected protein were full minimized by AMBER
111 12 [41]. The ff12SB force field [41] was used to model the proteins, while the fullerene atoms were
112 modeled as uncharged Lennard-Jones particles by using the CA atom type (sp2 aromatic carbon
113 parameter), also from the AMBER force field. The minimization was carried out with sander, using
114 the GB (Generalized Born) model [42] for the solvation and no cut-off for van der Waals and
115 electrostatic was used.

116 **MM-GBSA analysis.** In order to identify the residues responsible for the binding of the proteins
117 to C_{60} , we carried out a decomposition analysis of the optimized structure according to the MM-GBSA
118 scheme [35,36]. The per-residue decomposition analysis provides the contribution of the individual
119 amino acids to the binding.

120

121 **3. Results and discussions**

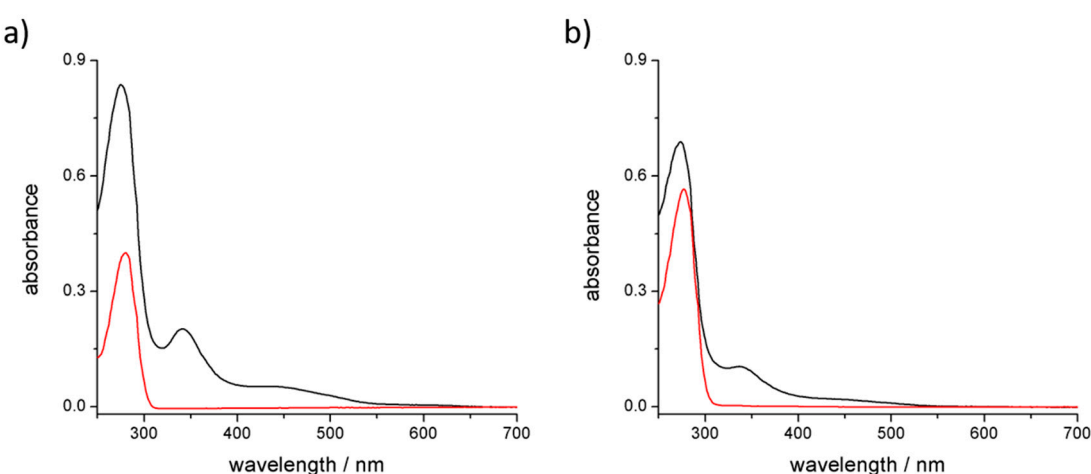
122 The ability of C_{60} to interact with proteins is a recent subject of investigation. Collectively, van
123 der Waals, hydrophobic and electrostatic interactions must cooperate to establish energetically
124 favorable interactions between a protein and a fullerene in order to allow the formation of a stable
125 complex [43]. Geometrical complementarity also plays a primary role to maximize the effect of the
126 stabilizing contributes [44]. Crucial for the understanding of protein-fullerene interactions is the
127 identification of the fullerene-binding site together with the possible subsequent proteins structural
128 modification [45]. It should also be further assessed if the interaction occurs between a single fullerene
129 with a single protein or if fullerenes clusters are surrounded by a number of proteins.

130

131 Pepsin ($pI = 2.2 - 3$) [46] and trypsin ($pI = 10.2 - 10.8$) [47] are proteins characterized by very
132 different values of isoelectric point, which makes one negatively and the other positively charged in
133 physiological conditions. Sonication of C_{60} with each protein was performed in acidic (pH 2), neutral,
134 and basic pH (pH 12) of unbuffered aqueous solutions. Pepsin was able to disperse fullerene in water
135 only at basic pH, where the protein is negatively charged, while trypsin showed the best
136 performances at acidic pH.

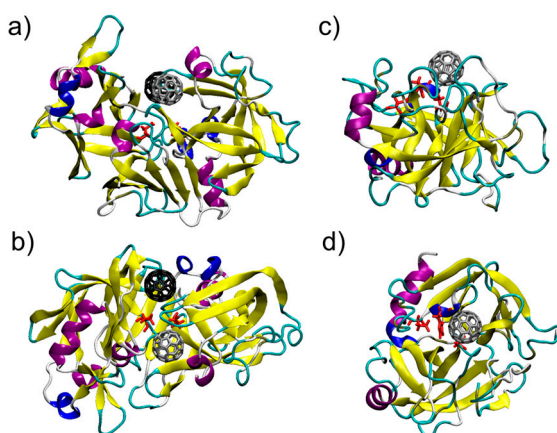
137 The two batches of hybrids were synthetized under optimized conditions. After sonication and
138 centrifugation, the supernatants were collected and characterized. UV-Vis spectra of the solutions
139 (Figure 1) show the diagnostic absorption bands of C_{60} at 341 nm and the overlap of C_{60} and protein
140 absorption bands between 260-290 nm. Based on the extinction coefficients of both components of the

141 adducts [48], the absorption spectra suggest a 1:1 stoichiometry between C₆₀ and trypsin, while 1:2
 142 stoichiometry can be estimated for the C₆₀ and pepsin complex. UV-Vis spectra also suggest that the
 143 presence of particle aggregates, observed prior to centrifugation, was completely removed since
 144 scattering is not exhibited.
 145



146
 147 **Figure 1.** UV-visible spectra of (a) C₆₀@trypsin (black line) and trypsin (red line); (b) C₆₀@pepsin (black line)
 148 and pepsin (red line).
 149
 150

151 *3.1. C₆₀@pepsin – C₆₀@trypsin, an atomistic view*



152
 153 **Figure 2.** Two perspectives of C₆₀@pepsin (a, b) and C₆₀@trypsin (c, d). In red, the catalytic residues of the
 154 two proteins.

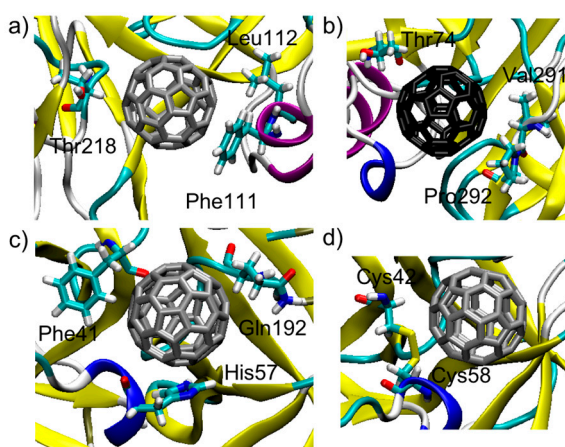
155 Surface complementarity between the proteins and the C₆₀ surface appears. The results of the docking
 156 protocol explain the stoichiometry observed by the UV-visible spectra. Pepsin is characterized by a
 157 dimeric interface region. In this region, two fullerene binding pockets are identifiable and are able to
 158 bind two C₆₀ cages (figure 2a and 2b). The binding between C₆₀ and pepsin is not surprising, since
 159 pepsin is an aspartic protease and structurally strongly correlates to HIV protease: fullerenes are well
 160 known inhibitors of HIV-1 protease [49–52]. In pepsin, as in the HIV protease, fullerenes block the
 161 large active site groove [49–52]. C₆₀ is also a known serine protease inhibitor [53], and in fact C₆₀ binds
 162 in the trypsin active site: a single, well defined binding pocket is identified by the docking protocol
 163 in this region (figure 2c and 2d). For the two C₆₀@protein hybrids tested here, MM-GBSA analysis of
 164 the structures in their optimized geometries provides a quantitative description of the C₆₀ binding
 165 pocket and identifies the more effectively interacting residues. Table 1 shows the 10 largest

166 interactions between the residues of the proteins and C₆₀. The three most interacting residue for
 167 binding pocket are represented in Figure 3a-c.

168 **Table 1.** Interaction energies (kcal mol⁻¹) of the top 10 residues interacting with C₆₀.
 169

C ₆₀ @Pepsin- Binding pocket 1	Phe 111 = -5.7	Leu 112 = -3.1	Thr 218 = -3.0	Ser 219 = -2.9	Thr 12 = -2.8
	Glu 13 = -2.8	Phe 117 = -2.6	Ile 30 = -2.5	Tyr 75 = -2.5	Thr 77 = -2.2
C ₆₀ @Pepsin- Binding pocket 2	Val 291 = -4.9	Thr 74 = -4.3	Pro 292 = -3.7	Tyr 75 = -3.4	Gly 76 = -2.7
	Met 289 = -1.4	Thr 293 = -1.3	Tyr 189 = -1.2	Asp 290 = -1.0	Leu 298 = -0.6
C ₆₀ @Trypsin	His 57 = -4.9	Phe 41 = -4.2	Gln 192 = -3.5	Cys 58 = -3.4	Cys 42 = -2.7
	Gly 193 = -1.8	Ser 195 = -1.7	Asp 194 = -0.8	Tyr 151 = -0.6	Leu 99 = -0.4

170



171

172 **Figure 3.** Top 3 residues interacting with C₆₀ in the (a) pepsin binding pocket 1, (b) pepsin binding pocket
 173 2; (c) Top 3 residues interacting with the C₆₀ in the trypsin binding pocket; (d) Interaction in the trypsin
 174 binding pocket between C₆₀ and a disulfide bridge (Cys42-Cys58).

175 From Table 1 and Figure 3 it appears that proteins are able to interact with C₆₀ via:

176 i) π - π stacking interactions that are established between aromatic residues (phenylalanine, tyrosine,
 177 histidine) and C₆₀ surface [25,54];

178 ii) Hydrophobic interactions (leucine, isoleucine, methionine, proline, glycine) that are established in
 179 water between aliphatic residues and C₆₀ surface [25];

180 iii) Surfactant-like interactions where amphiphilic residues (threonine, serine, aspartate) behave
 181 similarly to surfactants and solvate C₆₀. The hydrophobic aliphatic chains of these residues interact
 182 with C₆₀ surface, whereas the hydrophilic groups point out toward water [25,55,56].

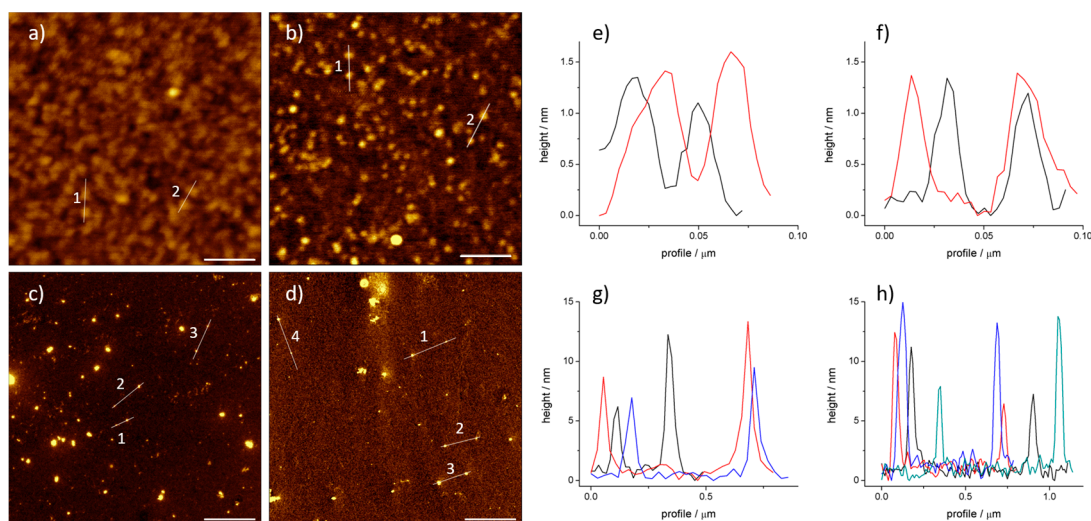
183 In the case of trypsin, of interest is the interaction between a disulfide bridge (Cys42-Cys58) and C₆₀
 184 (Figure 3d). This kind of interaction was recently highlighted by Hirano and coworkers for carbon
 185 nanotubes [57,58].

186 *3.2. AFM analysis of C₆₀@protein hybrids*

187 UV-Vis spectra and molecular modelling exhibit the expected stoichiometry between C₆₀ and
 188 proteins. They do not give information about the possible aggregation of the adducts. Atomic force
 189 microscopy is a direct technique to evaluate the size distribution of particles.

190 In Figure 4a, the C₆₀@trypsin hybrids are monomolecularly dispersed when deposited on a
 191 negatively charged mica surface. C₆₀@trypsin is positively charged, hence an electrostatic interaction
 192 takes place with the surface. The profile analysis (Figure 4b) of both C₆₀@trypsin and the trypsin
 193 reference (obtained in the same conditions) shows an average height of ~1.5 nm, which is slightly
 194 lower than the expected value. This behavior is a consequence of the strong electrostatic interaction,
 195 which squashes the proteins over the surface in order to maximize the attractive electrostatic contacts.
 196 Conversely, negatively charged pepsin hybrid (Figure 4c) shows an average height, which is slightly
 197 higher than the average size of the protein.

198 These results mainly originate from the combination of different forces: i) the pepsin tendency
 199 to self-associate; ii) the electrostatic repulsion between the pepsin and the surface, which reduces the
 200 number of interactions, as confirmed also by the small number of the particles deposited on the mica
 201 which repels the adduct. The AFM analysis demonstrates the absence of C₆₀@proteins aggregates, or
 202 nC₆₀ clusters dispersed by the proteins.



203
 204 **Figure 4.** AFM images of (a) C₆₀@trypsin; (b) trypsin; (c) C₆₀@pepsin; (d) pepsin. Profile analysis of the
 205 height of (e) C₆₀@trypsin; (f) trypsin; (g) C₆₀@pepsin; (h) pepsin. Scale bar (a,b) 100 nm; (c,d) 1 μm. The lines
 206 in the AFM provide the numbering of the AFM profiles: profile 1 in black, profile 2 in red, profile 3 in blue
 207 and profile 4 in green.

208

209 3.3. Stability of the complex in aqueous media

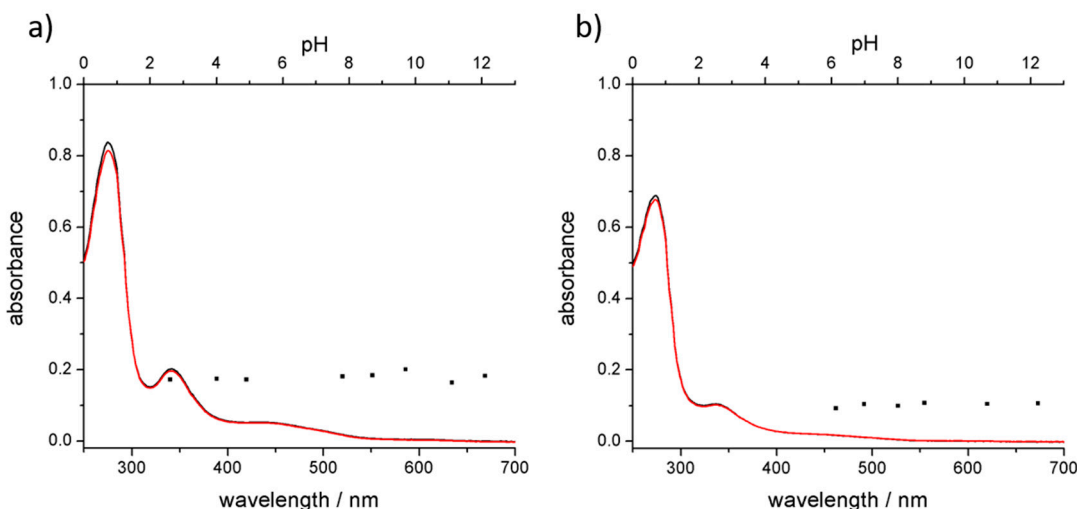
210 Compared to the chemical functionalization of the fullerenes, one of the advantages from the
 211 use of host-guest system is the possibility to tune the stability of the complex in aqueous media. The
 212 tuning can be achieved by acting only on the host system, that is the protein. Evaluating the behavior
 213 of C₆₀@proteins at different pH's and physiological conditions, it was found that the stability of the
 214 hybrid in aqueous media was completely governed by the protein. To understand if proteins pH
 215 sensitivity was retained, acid-basic titration was performed. Zeta potential and UV-Vis spectra were
 216 obtained. The correlation between zeta potential and pH gives information about the behavior of the
 217 complex for possible future *in vivo* experiments, since pH varies in different compartments of the
 218 organisms. Moreover, the greater the range of pH stability the wider the conditions for subsequent
 219 manipulation of the adduct. pH dependent zeta potential trends of C₆₀@trypsin and C₆₀@pepsin are
 220 shown in Figure 5.

221

222 **Figure 5.** Zeta potential of C_{60} @trypsin (in red) and C_{60} @pepsin (in blue) hybrids as a function of the
223 pH in aqueous solution. Standard deviations are shown in the error bars.

224 The isoelectric points (IEP) of both adducts resulted slightly shifted to values of pH's closer to
225 neutrality with respect to IEP of the pristine proteins. This phenomenon can be attributed to a
226 reduced accessibility to pH sensitive groups upon fullerene complexation. A further effect is related
227 to the local change of the environment polarity, which could slightly perturb the pKa of few charged
228 residues. For pH values closer to the IEP, the electrostatic repulsion between the proteins/adducts
229 becomes minimal. The stability of possible aggregates is governed only by steric hindrance.

230 For C_{60} @pepsin complexes at pH values close to IEP (2.7 and 4.5), aggregation phenomena
231 indeed occurred after few minutes. C_{60} @trypsin complexes did not aggregate also for pH values close
232 to the IEP. The maximum stability for individual C_{60} @pepsin complexes was obtained in neutral and
233 basic conditions. Absorption spectra performed on the same samples did not show changes of shape
234 and intensity (Figure 6) between the different samples. In both the cases, the complex resulted stable
235 for (at least) one week.



236

237 **Figure 6.** UV-Vis absorption spectra of (a) C_{60} @trypsin and (b) C_{60} @pepsin in water (black lines) and PBS
238 (red lines). Black dots represent the absorbance of fullerene diagnostic band (341 nm) of the hybrids at
239 different pH values (top axis).
240

241 Comparison of the absorption spectra of C₆₀@trypsin (Figure 6a) and C₆₀@pepsin (Figure 6b) in
242 water and PBS shows that the hybrids are stable also in physiologically relevant conditions
243 (represented by PBS). This is an important difference with other C₆₀ adducts, for instance fullerenes
244 dispersed by cyclodextrins rapidly precipitates when NaCl is added [59].

245 These results suggest that fine-tuning of the net charge of the complex is possible and therefore
246 it should also be possible to take advantage of the nature of each protein to create optimal C₆₀-protein
247 systems as a function of the pH. Tuning the net charge of the protein used to host the C₆₀ molecule it
248 is possible to governs its interactions with cellular and bacterial surface, controlling C₆₀ toxicity [60–
249 63].

250

251 **Acknowledgments:** This study was supported by the Italian Ministry of Education, University and Research
252 MIUR – SIR Programme no. RBSI149ZN9-BIOTAXI funded to M.C.

253 **Conflicts of Interest:** The authors declare no conflict of interest
254

255 **References**

256 1. Nakamura, E.; Isobe, H. Functionalized Fullerenes in Water. The First 10 Years of Their Chemistry,
257 Biology, and Nanoscience. *Acc. Chem. Res.* **2003**, *36*, 807–815, doi:10.1021/AR030027Y.

258 2. Goodarzi, S.; Da Ros, T.; Conde, J.; Sefat, F.; Mozafari, M. Fullerene: biomedical engineers get to revisit
259 an old friend. *Mater. Today* **2017**, *20*, 460–480, doi:10.1016/J.MATTOD.2017.03.017.

260 3. Castro, E.; Garcia, A. H.; Zavala, G.; Echegoyen, L. Fullerenes in biology and medicine. *J. Mater. Chem. B*
261 **2017**, *5*, 6523–6535, doi:10.1039/C7TB00855D.

262 4. Dellinger, A.; Zhou, Z.; Connor, J.; Madhankumar, A.; Pamujula, S.; Sayes, C. M.; Kepley, C. L.
263 Application of fullerenes in nanomedicine: an update. *Nanomedicine* **2013**, *8*, 1191–1208,
264 doi:10.2217/nnm.13.99.

265 5. Partha, R.; Conyers, J. L. Biomedical applications of functionalized fullerene-based nanomaterials. *Int. J.*
266 *Nanomedicine* **2009**, *4*, 261, doi:10.2147/IJN.S5964.

267 6. Bosi, S.; Da Ros, T.; Spalluto, G.; Prato, M. Fullerene derivatives: an attractive tool for biological
268 applications. *Eur. J. Med. Chem.* **2003**, *38*, 913–923.

269 7. Montellano, A.; Da Ros, T.; Bianco, A.; Prato, M. Fullerene C60 as a multifunctional system for drug and
270 gene delivery. *Nanoscale* **2011**, *3*, 4035, doi:10.1039/c1nr10783f.

271 8. Mroz, P.; Tegos, G. P.; Gali, H.; Wharton, T.; Sarna, T.; Hamblin, M. R. Fullerenes as Photosensitizers in
272 Photodynamic Therapy. In *Fullerenes as Photosensitizers in Photodynamic Therapy*; 2008; pp. 79–106.

273 9. Calvaresi, M.; Zerbetto, F. Baiting proteins with C60. *ACS Nano* **2010**, *4*, 2283–99, doi:10.1021/nn901809b.

274 10. Yang, S.-T.; Wang, H.; Guo, L.; Gao, Y.; Liu, Y.; Cao, A. Interaction of fullerol with lysozyme
275 investigated by experimental and computational approaches. *Nanotechnology* **2008**, *19*, 395101,
276 doi:10.1088/0957-4484/19/39/395101.

277 11. Chaudhuri, P.; Paraskar, A.; Soni, S.; Mashelkar, R. A.; Sengupta, S. Fullerol–Cytotoxic Conjugates for
278 Cancer Chemotherapy. *ACS Nano* **2009**, *3*, 2505–2514, doi:10.1021/nn900318y.

279 12. Bolksar, R. D. Gadolinium Endohedral Metallofullerene-Based MRI Contrast Agents. In; 2008; pp. 157–
280 180.

281 13. Da Ros, T. Twenty Years of Promises: Fullerene in Medicinal Chemistry. In *Twenty Years of Promises:*
282 *Fullerene in Medicinal Chemistry*; 2008; pp. 1–21.

283 14. Sharma, S. K.; Chiang, L. Y.; Hamblin, M. R. Photodynamic therapy with fullerenes *in vivo*: reality or a
284 dream? *Nanomedicine* **2011**, *6*, 1813–1825, doi:10.2217/nnm.11.144.

285 15. Mroz, P.; Tegos, G. P.; Gali, H.; Wharton, T.; Sarna, T.; Hamblin, M. R. Photodynamic therapy with
286 fullerenes. *Photochem. Photobiol. Sci.* **2007**, *6*, 1139, doi:10.1039/b711141j.

287 16. Guldi, D. M.; Hungerbuehler, H.; Asmus, K.-D. Redox and Excitation Studies with C60-Substituted
288 Malonic Acid Diethyl Esters. *J. Phys. Chem.* **1995**, *99*, 9380–9385, doi:10.1021/j100023a013.

289 17. Guldi, D. M.; Prato, M. Excited-State Properties of C60 Fullerene Derivatives. *Acc. Chem. Res.* **2000**, *33*,
290 695–703, doi:10.1021/AR990144M.

291 18. Hamano, T.; Okuda, K.; Mashino, T.; Hirobe, M.; Arakane, K.; Ryu, A.; Mashiko, S.; Nagano, T. Singlet
292 oxygen production from fullerene derivatives: effect of sequential functionalization of the fullerene core.
293 *Chem. Commun.* **1997**, 21–22, doi:10.1039/a606335g.

294 19. Ikeda, A. Water-soluble fullerenes using solubilizing agents, and their applications. *J. Incl. Phenom.*
295 *Macrocycl. Chem.* **2013**, *77*, 49–65, doi:10.1007/s10847-013-0319-9.

296 20. Dallavalle, M.; Leonzio, M.; Calvaresi, M.; Zerbetto, F. Explaining Fullerene Dispersion by using Micellar
297 Solutions. *ChemPhysChem* **2014**, *15*, 2998–3005, doi:10.1002/cphc.201402282.

298 21. Vance, S. J.; Desai, V.; Smith, B. O.; Kennedy, M. W.; Cooper, A. Aqueous solubilization of C60 fullerene
299 by natural protein surfactants, latherin and ranaspumin-2. *Biophys. Chem.* **2016**, *214–215*, 27–32,
300 doi:10.1016/J.BPC.2016.05.003.

301 22. Calvaresi, M.; Arnesano, F.; Bonacchi, S.; Bottoni, A.; Calò, V.; Conte, S.; Falini, G.; Fermani, S.; Losacco,
302 M.; Montalti, M.; Natile, G.; Prodi, L.; Sparla, F.; Zerbetto, F. C60@Lysozyme: direct observation by
303 nuclear magnetic resonance of a 1:1 fullerene protein adduct. *ACS Nano* **2014**, *8*, 1871–7,
304 doi:10.1021/nn4063374.

305 23. Calvaresi, M.; Zerbetto, F. Baiting Proteins with C60. *ACS Nano* **2010**, *4*, 2283–2299,
306 doi:10.1021/nn901809b.

307 24. Calvaresi, M.; Zerbetto, F. Fullerene sorting proteins. *Nanoscale* **2011**, *3*, 2873–2881,
308 doi:10.1039/c1nr10082c.

309 25. Calvaresi, M.; Zerbetto, F. The Devil and Holy Water: Protein and Carbon Nanotube Hybrids. *Acc. Chem.*
310 *Res.* **2013**, *46*, 2454–2463, doi:10.1021/ar300347d.

311 26. Nepal, D.; Geckeler, K. E. pH-Sensitive Dispersion and Debundling of Single-Walled Carbon Nanotubes:
312 Lysozyme as a Tool. *Small* **2006**, *2*, 406–412, doi:10.1002/smll.200500351.

313 27. Matsuura, K.; Saito, T.; Okazaki, T.; Ohshima, S.; Yumura, M.; Iijima, S. Selectivity of Water-Soluble
314 Proteins in Single-Walled Carbon Nanotube Dispersions. *Chem. Phys. Lett.* **2006**, *429*, 497.

315 28. Nepal, D.; Geckeler, K. E. Proteins and Carbon Nanotubes: Close Encounter in Water. *Small* **2007**, *3*,
316 1259–1265, doi:10.1002/smll.200600511.

317 29. Karajanagi, S. S.; Yang, H.; Asuri, P.; Sellitto, E.; Dordick, J. S.; Kane, R. S. Protein-Assisted Solubilization
318 of Single-Walled Carbon Nanotubes. *Langmuir* **2006**, *22*, 1392–1395.

319 30. Joseph, D.; Tyagi, N.; Ghimire, A.; Geckeler, K. E. A direct route towards preparing pH-sensitive

320 graphene nanosheets with anti-cancer activity. *RSC Adv.* **2014**, *4*, 4085–4093, doi:10.1039/C3RA45984E.

321 31. Bhattacharjee, S. DLS and zeta potential – What they are and what they are not? *J. Control. Release* **2016**,
322 235, 337–351, doi:10.1016/J.JCONREL.2016.06.017.

323 32. Ge, C. Binding of blood proteins to carbon nanotubes reduces cytotoxicity. *Proc. Natl Acad. Sci. USA* **2011**,
324 108, 16968–16973.

325 33. Walczyk, D.; Bombelli, F. B.; Monopoli, M. P.; Lynch, I.; Dawson, K. A. What the Cell “Sees” in
326 Bionanoscience. *J. Am. Chem. Soc.* **2010**, *132*, 5761–5768, doi:10.1021/ja910675v.

327 34. Soldà, A.; Cantelli, A.; Di Giosia, M.; Montalti, M.; Zerbetto, F.; Rapino, S.; Calvaresi, M. C60@lysozyme:
328 a new photosensitizing agent for photodynamic therapy. *J. Mater. Chem. B* **2017**, *1757*, 525–534,
329 doi:10.1039/C7TB00800G.

330 35. Genheden, S.; Ryde, U. The MM/PBSA and MM/GBSA methods to estimate ligand-binding affinities.
331 *Expert Opin. Drug Discov.* **2015**, *10*, 449–461, doi:10.1517/17460441.2015.1032936.

332 36. Wang, C.; Greene, D.; Xiao, L.; Qi, R.; Luo, R. Recent Developments and Applications of the MMPBSA
333 Method. *Front. Mol. Biosci.* **2017**, *4*, 87, doi:10.3389/fmolb.2017.00087.

334 37. Schneidman-Duhovny, D.; Inbar, Y.; Polak, V.; Shatsky, M.; Halperin, I.; Benyamin, H.; Barzilai, A.;
335 Dror, O.; Haspel, N.; Nussinov, R.; Wolfson, H. J. Taking geometry to its edge: Fast unbound rigid (and
336 hinge-bent) docking. *Proteins* **2003**, *52*, 107–112, doi:10.1002/prot.10397.

337 38. Andrusier, N.; Nussinov, R.; Wolfson, H. J. FireDock: Fast interaction refinement in molecular docking.
338 *Proteins* **2007**, *69*, 139–159, doi:10.1002/prot.21495.

339 39. Kingsford, C. L.; Chazelle, B.; Singh, M. Solving and analyzing side-chain positioning problems using
340 linear and integer programming. *Bioinformatics* **2005**, *21*, 1028–1039, doi:10.1093/bioinformatics/bti144.

341 40. Zhang, C.; Vasmatzis, G.; Cornette, J. L.; DeLisi, C. Determination of atomic desolvation energies from
342 the structures of crystallized proteins. *J. Mol. Biol.* **1997**, *267*, 707–726, doi:10.1006/jmbi.1996.0859.

343 41. Case, D. A.; Darden, T. A.; Cheatham, E. T.; Simmerling, C. L.; Wang, J.; Duke, R. E.; Luo, R.; Walker, R.
344 C.; Zhang, W.; Merz, K. M.; Roberts, B.; Hayik, S.; Roitberg, A.; Seabra, G.; Swails, J.; Götz, A. W.;
345 Kolossváry, I.; F.Wong, K.; Paesani, F.; Vanicek, J.; M.Wolf, R.; Liu, J.; Wu, X.; Brozell, S. R.; Steinbrecher,
346 T.; Gohlke, H.; Cai, Q.; Ye, X.; Wang, J.; Hsieh, M.-J.; Cui, G.; Roe, D. R.; Mathews, D. H.; Seetin, M. G.;
347 Salomon-Ferrer, R.; C. Sagui, V. B.; Luchko, T.; Gusarov, S.; Kovalenko, A.; Kollman, P. A. AMBER 12
348 2012.

349 42. Tsui, V.; Case, D. A. Theory and applications of the generalized born solvation model in macromolecular
350 simulations. *Biopolymers* **2000**, *56*, 275–291, doi:10.1002/1097-0282(2000)56:4<275::AID-
351 BIP10024>3.0.CO;2-E.

352 43. Calvaresi, M.; Bottone, A.; Zerbetto, F. Thermodynamics of Binding Between Proteins and Carbon
353 Nanoparticles: The Case of C60@Lysozyme. *J. Phys. Chem. C* **2015**, *119*, 28077–28082,

354 doi:10.1021/acs.jpcc.5b09985.

355 44. Calvaresi, M.; Furini, S.; Domene, C.; Bottoni, A.; Zerbetto, F. Blocking the Passage: C60 Geometrically
356 Clogs K⁺ Channels. *ACS Nano* **2015**, *9*, 4827–4834, doi:10.1021/nn506164s.

357 45. Trozzi, F.; Marforio, T. D.; Bottoni, A.; Zerbetto, F.; Calvaresi, M. Engineering the Fullerene-protein
358 Interface by Computational Design: The Sum is More than its Parts. *Isr. J. Chem.* **2017**, *57*, 547–552,
359 doi:10.1002/ijch.201600127.

360 46. Jonsson, M. Isoelectric spectra of native and base denatured crystallized swine pepsin. *Acta Chem. Scand.*
361 **1972**, *26*, 3435–40.

362 47. Walsh, K. A. Trypsinogens and trypsins of various species. *Methods Enzymol.* **1970**, *19*, 41–63,
363 doi:10.1016/0076-6879(70)19006-9.

364 48. Chen, Z.; Westerhoff, P.; Herckes, P. Quantification of C60 fullerene concentrations in water. *Environ.*
365 *Toxicol. Chem.* **2008**, *27*, 1852, doi:10.1897/07-560.1.

366 49. Friedman, S. H.; DeCamp, D. L.; Sijbesma, R. P.; Srdanov, G.; Wudl, F.; Kenyon, G. L. Inhibition of the
367 HIV-1 protease by fullerene derivatives: model building studies and experimental verification. *J. Am.*
368 *Chem. Soc.* **1993**, *115*, 6506–6509, doi:10.1021/ja00068a005.

369 50. Sijbesma, R.; Srdanov, G.; Wudl, F.; Castoro, J. A.; Wilkins, C.; Friedman, S. H.; DeCamp, D. L.; Kenyon,
370 G. L. Synthesis of a fullerene derivative for the inhibition of HIV enzymes. *J. Am. Chem. Soc.* **1993**, *115*,
371 6510–6512, doi:10.1021/ja00068a006.

372 51. Gian Luca Marcorin, †; Tatiana Da Ros, †; Sabrina Castellano, †; Giorgio Stefancich, †; Irena Bonin, ‡;
373 Stanislav Miertus, ‡ and; Maurizio Prato*, † Design and Synthesis of Novel [60]Fullerene Derivatives as
374 Potential HIV Aspartic Protease Inhibitors. **2000**, *2*, 3955–3958, doi:10.1021/OL000217Y.

375 52. Schuster, D. I.; Wilson, S. R.; Schinazi, R. F. Anti-human immunodeficiency virus activity and
376 cytotoxicity of derivatized buckminsterfullerenes. *Bioorg. Med. Chem. Lett.* **1996**, *6*, 1253–1256,
377 doi:10.1016/0960-894X(96)00210-7.

378 53. Tokuyama, H.; Yamago, S.; Nakamura, E.; Shiraki, T.; Sugiura, Y. Photoinduced biochemical activity of
379 fullerene carboxylic acid. *J. Am. Chem. Soc.* **1993**, *115*, 7918–7919, doi:10.1021/ja00070a064.

380 54. Iwashita, K.; Shiraki, K.; Ishii, R.; Tanaka, T.; Hirano, A. Liquid Chromatographic Analysis of the
381 Interaction between Amino Acids and Aromatic Surfaces Using Single-Wall Carbon Nanotubes.
382 *Langmuir* **2015**, *31*, 8923–8929, doi:10.1021/acs.langmuir.5b02500.

383 55. Calvaresi, M.; Hoefinger, S.; Zerbetto, F. Probing the Structure of Lysozyme-Carbon-Nanotube Hybrids
384 with Molecular Dynamics. *Chem. - A Eur. J.* **2012**, *18*, 4308–4313, doi:10.1002/chem.201102703.

385 56. Hirano, A.; Tanaka, T.; Kataura, H.; Kameda, T. Arginine Side Chains as a Dispersant for Individual
386 Single-Wall Carbon Nanotubes. *Chem. - A Eur. J.* **2014**, *20*, 4922–4930, doi:10.1002/chem.201400003.

387 57. Hirano, A.; Kameda, T.; Wada, M.; Tanaka, T.; Kataura, H. Carbon Nanotubes Facilitate Oxidation of
388 Cysteine Residues of Proteins. *J. Phys. Chem. Lett.* **2017**, *8*, 5216–5221, doi:10.1021/acs.jpclett.7b02157.

389 58. Hirano, A.; Kameda, T.; Sakuraba, S.; Wada, M.; Tanaka, T.; Kataura, H. Disulfide bond formation of
390 thiols by using carbon nanotubes. *Nanoscale* **2017**, *9*, 5389–5393, doi:10.1039/c7nr01001j.

391 59. Shigeru Deguchi; Rossitza G. Alargova, A.; Tsuji, K. Stable Dispersions of Fullerenes, C₆₀ and C₇₀, in
392 Water. Preparation and Characterization. *Langmuir* **2001**, *17*, 6013–6017, doi:10.1021/LA010651O.

393 60. Tang, Y. J.; Ashcroft, J. M.; Chen, D.; Min, G.; Kim, C.-H.; Murkhejee, B.; Larabell, C.; Keasling, J. D.;
394 Chen, F. F. Charge-Associated Effects of Fullerene Derivatives on Microbial Structural Integrity and
395 Central Metabolism. *Nano Lett.* **2007**, *7*, 754–760, doi:10.1021/nl063020t.

396 61. Deryabin, D. G.; Efremova, L. V.; Vasilchenko, A. S.; Saidakova, E. V.; Sizova, E. A.; Troshin, P. A.;
397 Zhilenkov, A. V.; Khakina, E. A. A zeta potential value determines the aggregate's size of penta-
398 substituted [60]fullerene derivatives in aqueous suspension whereas positive charge is required for
399 toxicity against bacterial cells. *J. Nanobiotechnology* **2015**, *13*, 50, doi:10.1186/s12951-015-0112-6.

400 62. Deryabin, D. G.; Davydova, O. K.; Yankina, Z. Z.; Vasilchenko, A. S.; Miroshnikov, S. A.; Kornev, A. B.;
401 Ivanchikhina, A. V.; Troshin, P. A. The Activity of [60]Fullerene Derivatives Bearing Amine and
402 Carboxylic Solubilizing Groups against *Escherichia coli*: A Comparative Study. *J. Nanomater.* **2014**, *2014*,
403 1–9, doi:10.1155/2014/907435.

404 63. Tegos, G. P.; Demidova, T. N.; Arcila-Lopez, D.; Lee, H.; Wharton, T.; Gali, H.; Hamblin, M. R. Cationic
405 fullerenes are effective and selective antimicrobial photosensitizers. *Chem. Biol.* **2005**, *12*, 1127–35,
406 doi:10.1016/j.chembiol.2005.08.014.